

EFFECT OF NANOCCLAY ON THE ATOM TRANSFER RADICAL POLYMERIZATION OF LAURYL METHACRYLATE

Pravin Kumar Srivastava

Department of Chemistry Sanjay Gandhi (P.G.) College, Meerut, INDIA

Abstract: Role of nanoclay as additives in Atom transfer Radical Polymerization was observed as it leads to a remarkable increase in polymerization rate without losing control. Two parameters, viz., the dispersion time of clay in monomer prior to polymerization and extent of clay loading are found to have a positive effect on the kinetics of polymerization.

Keywords: Atom transfer radical polymerization (ATRP), N-(*n*-octyl)-2-pyridinemethanimine, Cloisite 30B Gel permeation chromatography (GPC)

I. INTRODUCTION

The development of controlled/living radical polymerization (CLRP) for the synthesis of polymers with controlled architecture, molecular weight and molecular weight distribution is among the most significant accomplishments in polymer science^{1,2}. Among three kinds of CLRP methods, the atom transfer radical polymerization (ATRP) is one of the most successful methods. ATRP is based on a fast dynamic equilibrium established between the dormant species and active radicals. However, polymerization rate in any controlled/living radical polymerization is significantly low than that of the conventional free-radical polymerization, due to low concentration of active radical species ($\sim 10^{-8}$ - 10^{-7} M) so as to avoid termination resulting in controlled polymerization. It was well reported that solvents such as acetonitrile³, ethylene carbonate⁴ or water^{5,6} and additives such as carboxylic acid⁷ or phenol⁸ can act as accelerators in ATRP. Even metal alkoxides are effective in increasing the polymerization rate as well as narrowing the MWDs of the produced polymers

Recently, development of polymer/clay nanocomposites is one of the most important topic globally in the field of polymer research. In-situ ATRP technique has also been used to produce polymer/layered silicate nanocomposites^{9, 10-13} with considerable improvements in the properties of polymer¹⁴⁻¹⁷.

After this study, several groups expanded the use of ATRP to prepare nanocomposites that contained polystyrene¹⁸, poly(butyl acrylate)¹⁹, poly(methyl methacrylate)^{14,18} and poly(2-hydroxyethyl methacrylate)¹⁹. The interesting role of nanoclay in the atom transfer radical polymerization of ethyl acrylate (EA) has been reported by Bhowmick et al.²⁰. Results show that the use of nanoclay in the ATRP of EA leads to a significant increase in the polymerization rate. Semsarzadeh et al²¹ has also reported a significant increase in polymerization rate of MMA in presence of nanoclay (Cloisite 30B). The increase in polymerization rate was attributed to the activated conjugated $>C=C<$ bond of MMA monomer via interaction between the carbonyl group of MMA monomer and the hydroxyl moiety (Al-O-H) of nanoclay as well as to the positive effect of nanoclay on the dynamic equilibrium between the active (macro)radicals and dormant species. However, in case of styrene monomer (a non coordinative monomer with nanoclay), polymerization rate decreased slightly in the presence of nanoclay.

Controlled polymerization of higher alkyl methacrylates by ATRP method is difficult due to the insolubility of catalyst. Since both monomer and the polymer formed are hydrophobic in nature, however Cu(I)Br/ Cu(II)Br catalysts are polar in nature therefore catalyst gets precipitated. In most cases, ATRP of higher methacrylates was done in the presence of solvent. Haddelton et al. examined the ATRP of *n*-butyl, *n*-hexyl and *n*-nonyl methacrylate using EBiB as initiator, CuBr as catalyst and *N*-(*n*-butyl)-2-pyridinemethanimine as ligand in xylene at 95°C. Choudhary et al.²³ reported the bulk and solution polymerization of LMA via the ATRP method using EBiB as initiator, CuBr as catalyst and *N*-(*n*-propyl)[PPMI] *n*-hexyl[HPMI]/*n*-octyl[OPMI] -2-pyridinemethanimine as ligands. In the polymerization of LMA, better control was observed when OPMI was used as ligand. OPMI was found to be very efficient ligand for homogeneous bulk and solution polymerization of higher alkyl methacrylates.

In the extension of above work, we describe the atom transfer radical polymerization of LMA at 95°C in solution (toluene) in presence of nanoclay using CuBr as catalyst, N-(n-octyl)-2-pyridinemethanimine [OPMI] as ligand and EBiB as initiator. This paper describes the effect of organically modified clay particle on the kinetics of LMA. Various parameters were taken into consideration like dispersion time of clay and amount of clay loading on the kinetics and synthesis of polymer clay nanocomposites.

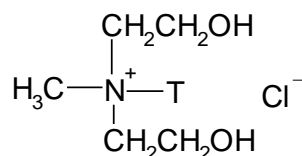
II. EXPERIMENTAL

2.1 Materials

Lauryl methacrylate, LMA (Aldrich, USA, 96%) was purified by washing with 5% aqueous NaOH solution, followed by washing with water till neutral and then dried over anhydrous CaCl₂. Finally it was distilled under vacuum and stored in refrigerator below 5°C.

Cloisite 30B, a montmorillonite treated by an ion-exchange reaction with the surfactant methyl tallow bis-2-hydroxy ethyl quaternary ammonium (Southern Clay Products, Gonzales, TX), was dried in a vacuum oven (60°C, 40 mmHg) before use.

Nanoclay (Cloisite 30B) was obtained from Southern Clay Products, Texas, USA having XRD peak for (001) plane, 2 θ (degree) at 4.8 and d-spacing at 1.85 nm. It is organically modified with MT₂EtOH: methyl, tallow (~ 65% C 18; ~30% C16 ~5% C14) like oleic or linoleic acid), bis-2-hydroxyethyl, quaternary ammonium structure given below.



Copper bromide, (Aldrich USA, 98%) was purified by stirring in glacial acetic acid under nitrogen followed by filtration, washing with dry ethanol and dried at 100°C.

Ethyl-2-bromo-isobutyrate (EBiB) (Aldrich USA, 98%) was used as received.

Toluene (Merck) was dried and purified by refluxing with sodium and benzophenone under nitrogen followed by distillation.

2.2 Polymerization of LMA in Presence of Nanoclay

A dry schlenk tube was filled with required amounts of nanoclay and monomer LMA (5.97ml, 20.4 m mol), (already degassed by purging with nitrogen for more than 30 min before use) under nitrogen atmosphere at room temperature. CuBr (0.0585g, 0.408 mmol), OPMI (0.2227g, 1.02 m mol), 2ml of toluene was added in that order. The reaction mixture was purged with nitrogen for 15 minutes to remove traces of oxygen.

The tube was degassed three times by repeated freeze/ vacuum/ thaw cycles and finally evacuated and back filled with nitrogen. The initiator ethyl-2-bromoisobutyrate EBiB (0.0585ml, 0.408mmol) was added to the reaction mixture in the schlenk tube via dry and purified syringe. The reaction mixture was then placed in a preheated oil bath at 95°C. The polymerization was stopped at a desired time by cooling the tube in ice water. The reaction mixture was diluted with toluene and passed through a short neutral alumina column to remove the catalyst. The polymer was precipitated with methanol. The polymer was then dried under vacuum for 24h at 60°C and yield was determined gravimetrically.

For kinetic studies, polymerization of LMA was carried out using the same procedure as reported above and 1ml of reaction mixture was withdrawn at definite time for the analysis of conversion and out of this sample small portion after dilution with THF was centrifuged. The supernatant solution was filtered using 0.2 μ PTFE filter before injection for the analysis of molecular weight and molecular weight distribution. In the second set of experiments, nanoclay was dispersed in monomer and stirred for 1h, 10h, 20h and the polymerization was done using the same procedure as reported above. To investigate the effect of dispersion time, the amount of nanoclay and other polymerization conditions were kept constant.

We also prepared the samples by polymerizing LMA in presence of varying amounts of clay ranging from 2-6% w/w. The PLMA samples having 0, 2, 4, and 6% of nanoclay have been designated as PLMA followed by numerical suffix representing the amount of nanoclay. For example PLMA having 0, 2, 4 and 6% of nanoclay have been designated as PLMA-0, PLMA-2, PLMA-4 and PLMA-6 respectively.

Samples prepared after swelling nanoclay [2% (w/w)] in monomer before polymerization have been designated as PLMA-2 followed by numerals within parenthesis representing the dispersion time. For example, PLMA-2 prepared after dispersion of nanoclay for 0h, 10h and 20h have been designated as PLMA-2[0], PLMA-2[10] and PLMA-2[20] respectively

III. CHARACTERIZATION

3.1 Structural Characterization

FT-IR spectra were recorded as thin films using a Nicolet FTIR spectrophotometer (Waltham, MA). NMR spectra were recorded on a Bruker spectrosopin DPX 300 spectro-meter (Fallenden, Switzerland) using CDCl_3 as a solvent and tetramethyl silane as an internal standard.

3.2 Molecular Characterization

Waters (1525) gel permeation chromatograph (Milford, MA) equipped with styragel (HR-3 and HR-4, 7.8x 300 mm) columns along with Evaporating Light Scattering Detector (ELSD-2420) was used to determine the molecular weight and molecular weight distribution in polymers. For calibration, polystyrene standards (Shodex Standards SL-105, Japan) having molecular weight of 197,000, 51,000, 13,900 and 2100 were used. THF was used as solvent at a flow rate of 1 ml/min.

3.3 Thermal Characterization

TA 2100 thermal analyzer, was used for recording thermogravimetric (TG) /derivative thermogravimetric (DTG) traces in nitrogen atmosphere over the temperature range of 50-800°C at a heating rate of 20°C/ min. A sample size of 10 ± 5 mg was used in each experiment.

3.4 Morphological Characterization

Bulk morphology of nanocomposites was studied using a high resolution transmission electron microscope (JEOL 2000) operated at an accelerated voltage of 200 kV. Sample was prepared by dissolving the polymer in THF and a drop of solution was poured on the carbon coated copper grid and then dried in vacuum. X-ray diffraction (XRD) patterns were recorded on a PANalytical instrument, model number PW3040/60 X'pert PRO (Netherlands) using Ni filtered $\text{CuK}\alpha$ radiation ($\lambda=0.154$ nm). The voltage and the current of X-ray were 40kV and 30 mA respectively. The samples were scanned at a rate of 1°/min from 3° to 10° of 2θ .

IV. RESULTS AND DISCUSSION

4.1 Effect of Nanoclay as Additive on the Polymerization of LMA using ATRP

Choudhary et. al.²³ investigated systematically the effect of the length of alkyl group in ligand on the polymerization of LMA using CuBr as catalyst and EBiB as initiator. It was observed that OPMI ligand used for the polymerization of LMA resulted in homogeneous system at higher percentage conversion and gave polymer with controlled molecular weight and PDI. However, when OPMI was used as ligand, % conversion was lower due to the higher solubility of catalyst which facilitates the backward reaction resulting in low concentration of reactive radical. In order to enhance the polymerization, we have to investigate systematically the effect of nanoclay on the polymerization of LMA.

This was chosen on the basis of literature which clearly showed the beneficial effect of nanoclay on the polymerization of ethyl acrylate. Figure 1 shows the plot of $\ln[M]_0/[M]$ vs time for the polymerization of LMA using ATRP in the absence and presence of varying amounts of nanoclay. Monomer conversion increases with time, however at any given time it was higher in the presence of clay which increased with increasing amounts of clay. We investigated systematically the effect of nanoclay and the dispersion time on the polymerization of LMA and the results are discussed in the following text.

4.3 Effect of Clay Content

In order to investigate the effect of clay content on the homopolymerization of LMA, the clay content was taken as 2, 4 and 6%, all other parameter such as dispersion time (20h), M: CuBr: EBiB: OPMI [50: 1: 1: 2.5] temperature [95°C] in toluene as solvent and time [2h] were kept constant. Percentage conversion was determined after terminating the polymerization after 2h and the results are summarized in Table 1. In a given time, it was observed that % conversion increased from 15% [in absence of clay] to 25, 54 and 80% in presence of 2, 4 and 6% nanoclay respectively. These results clearly show that the presence of clay enhances the rate of polymerization. Similar behavior has also been reported by Bhowmick et al in the polymerization of ethyl acrylate in presence of clay. This could be due to coordination of Al atom of nanoclay with $>\text{C}=\text{O}$ group of ethyl acrylate monomer²²

Table 1: Effect of clay content on % conversion (dispersion time 20h)

Sample Designation*	Clay content (wt%)	Dispersion time (in min)	Conversion [%]	Mn _{GPC} (x 10 ⁻³) gmol ⁻¹	PDI
PLMA-0	0	-	15	2.22	1.30
PLMA-2 [20]	2	120	25	3.70	1.48
PLMA-4 [20]	4	120	54	7.54	1.88
PLMA-6 [20]	6	120	80	12.24	2.12

*Numerals 2, 4 and 6 represent nanoclay content; Numerals 20 within parenthesis represent dispersion time.

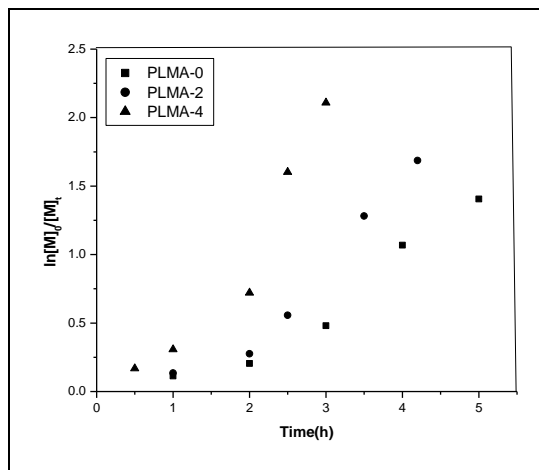


Figure .1: Plot of $\ln [M]_0 / [M]_t$ vs time for ATRP of LMA in toluene at 95°C [mol ratio of LMA: EBiB: CuBr: OPMI 50:1:1:2.5] in the absence/ presence of varying amounts of nanoclay.

4.2 Effect of Dispersion Time:

In the second set of experiments, we looked at the time of clay dispersion in monomer before polymerization on the kinetics of polymerization of LMA. For this purpose, the clay content was kept constant i.e., 2% (w/w) and the time for dispersion of nanoclay in monomer was varied as 0, 10 and 20h. In the preparation of PLMA-2[0], monomer, nanoclay, toluene, CuBr/ EBiB/ OPMI were mixed as mentioned in experimental section and polymerization was done at 95°C for 2h in the next case first 2% nanoclay was mixed with monomer and stirred for a given time (10h or 20h) and the polymerization was done keeping all the polymerization conditions constant i.e. time (2h), temperature 95°C CuBr: EBiB: OPMI 1: 1: 2.5 in toluene [as solvent]. The polymerization was terminated after 2h and % conversion was determined gravimetrically. Percent conversion increased dramatically with increase in dispersion time. For example, 22% conversion was observed in the presence of clay (after 1h of dispersion) which increased to 50% (after 10h of dispersion) and 80% (after 20h of dispersion). Figure 5.2 show the plot of % conversion vs dispersion time in case of sample PLMA-2.

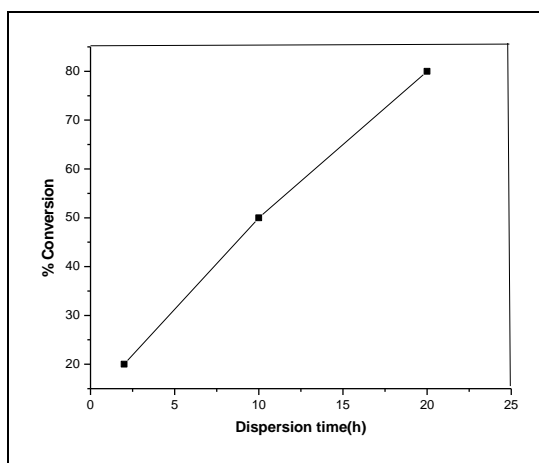


Figure 2: Plot of dispersion time prior to polymerization on the % conversion in sample PLMA-2

The increase in the polymerization rate of LMA in presence of organically modified nanoclay (Cloisite 30B) could be due to the presence of long chain hydrocarbon i.e. methyl tallow which is similar to the side chain of LMA monomer which might have facilitated the penetration of monomer in the galleries nanoclay. Therefore, with increase in swelling time, more monomer penetrates into the organophilic interlayer region and thus the concentration of LMA increases inside the gallery spacing tremendously (as evidenced by the enhancement in d-spacing, by Wide Angle X-ray Diffraction analysis). This might have facilitated the rate of polymerization. Similar kind of observation has been reported in literature ¹² that when the clay shows good compatibility or interaction with monomer, a significant swelling of the clay galleries by monomer is obtained.

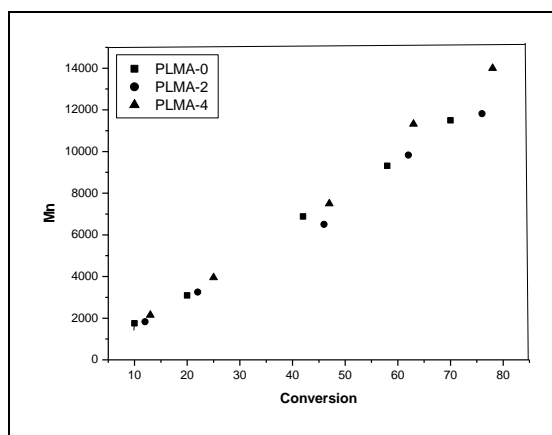


Figure .3: Plot of number average molecular weight (Mn GPC) vs. percent conversion for polymerization of LMA by ATRP in toluene at 95°C in the presence of varying amount of clay [mole ratio of LMA: EBiB: CuBr: OPMI 50:1:1:2.5].

The above kinetics and GPC results shows that nanoclay (Cloisite 30B) acts as an additive has a beneficial effect on the polymerization of LMA using ATRP. The time was reduced significantly in the presence of nanoclay to attain higher percent conversion. However the drawback of such polymerization systems is that it was better controlled when small amounts of nanoclay i.e. ~2% w/w was used as an additive whereas at clay loading of 6% (w/w), polymerization rate was enhanced significantly but with a poor control leading to higher PDI. Figure 3 shows the GPC results of the resultant polymer sample taken at different intervals and monomer conversions. Molecular weight (Mn) increases linearly with conversion which confirms the living nature of polymerization, however polydispersity index (PDI) is little broader which increases with increase in clay amount. Lowest molecular weight distribution is achieved in the polymer, PLMA-2 (1.48), PLMA-4 (1.88) and in the case of PLMA-6, there is very fast polymerization rate that renders loss of control over polymerization and the possibility of side reactions leads to higher PDI value (2.12) In all cases the molecular weight calculated by GPC was higher than the theoretically calculated molecular weight. The reason for the higher molecular weight (Mn_{GPC}) observed than calculated could be due to the difference in hydrodynamic volume of PLMA and PS standards which has been used for calibration.

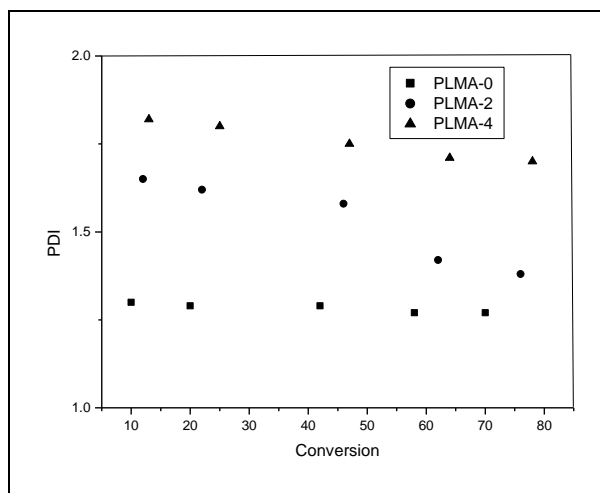


Figure.4: Plot of poly-dispersity index (PDI) vs. percent conversion for polymerization of LMA by ATRP at 95°C in presence of varying amount of clay [mol ratio of LMA: EBiB:CuBr: OPMI 50:1:1:2.5].

4.4 Mechanism:

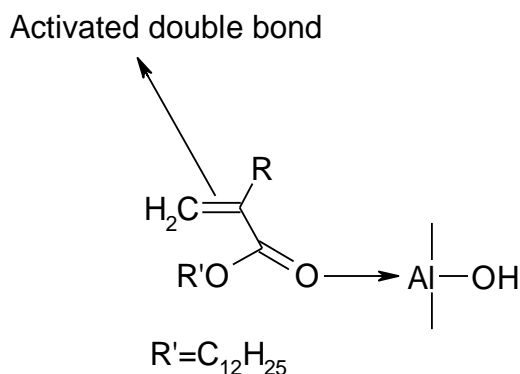
In-depth research was carried out to understand the underlying reaction mechanism.

Nanoclays belong to the general family of 2:1 layered phyllosilicates. Their crystal structure consists of layers made up of two tetrahedrally coordinated silicon atoms fused to an edge shared octahedral sheet of Al-(OH)₃. Stacking of the layers leads to a regular van der Waals gap called the interlayer or gallery. In nanoclays, clay surfaces are rendered organophilic on substitution of alkali or alkaline earth cations situated inside this interlayer spacing by long chain alkyl ammonium ions, resulting in a larger gallery spacing (e.g., 1.85 nm in Cloisite 30B, compared to 1.17 nm in unmodified clay, Cloisite Na⁺).

The lyotropic series²⁷ (for ion exchange of clay) indicates that the transition metals like Cu⁺ are not a good exchangeable cation for NH₄⁺, attached to the organic surfactant moiety, unless some special conditions are maintained (for example, lowering in surface potential etc., by using some external agents). Hence, it might be argued that during polymerization, there is a very less probability of cation exchange phenomena (Cu⁺ for NH₄⁺) to occur. This consequently prevents the release of surfactants and thereby modification of the coordination of Cu⁺ in polymerization is hindered. A similar mechanism can be postulated in the current polymerization system, where clay provides the negative charge surface and the active hydroxyl group (present on the surface as well as in the modifier) imparts polar character in the reaction medium, thereby encouraging the generation of active ionic intermediate species.

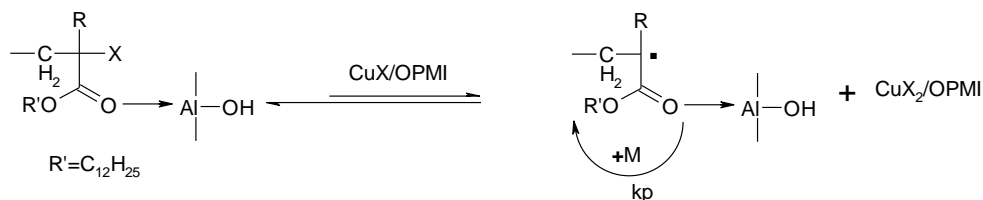
It has been reported previously that the use of polar solvents or polar additives, especially using those having an active hydroxyl group, e.g., phenol, carboxylic acid, water etc., have acceleration effects in ATRP^{3, 5, 6, 17} due to an improvement in radical activation rate and a decrease in the radical recombination rate. Matyjaszewski et al.^{9, 4} proposed the generation of more reactive [CuI(bpy)₂]⁺ complex with a halide counterion as the intermediate species in a polar medium in contrast to the neutral binuclear complex, formed in conventional ATRP. It has also been reported that a negatively charged surface could concentrate positively charged catalysts (i.e., Cu ions) and subsequently enhance the chain growth rate¹⁴.

Furthermore, a recent report has shown²¹ that organically modified nanoclay having Al atom in nanoclay that coordinate with >C=O group of ethyl acrylate monomer (EA) have a significant increase in the homopolymerization rate. Similarly presence of nanoclay (Cloisite 30B) has a significant and accelerating effect on the MMA polymerization. Therefore we can propose that the accelerating effect of nanoclay in the polymerization of LMA monomer using ATRP technique could be due to the formation of co-ordinate bond between >C=O group of LMA and layered aluminium silicate layers that in turn activate the attack of free radical on double bond and hence enhances the rate of polymerization. Amount of clay content is not only enhancing the rate of reaction however dispersion time also play important role on the polymerization. This results in increasing the rate of initiation and propagation, thereby enhancing the rate of polymerization. With increase in dispersion time, more LMA molecules penetrate the intergallery spacing in nanoclay and hence promote the polymerization rate.



Reaction Scheme .1 Schematic representation of coordination of clay with monomer

This interaction of >C=O with Al in nanoclay not only activate the double bond of LMA monomer for the attack of free radical, however it also affect dynamic equilibrium of activation-deactivation cycle in ATRP (reaction scheme-2). The >Al-O-H group of nanoclay interacts with the >C=O group of the dormant species (PLMA-Br); thereby activating the C-Br bond next to the ester carbonyl bond which facilitate further halogen transfer from dormant species to metal complex.



Reaction Scheme 2: Effect of NanoClay on the mechanism of ATRP of LMA

This interaction results in increasing the rate of initiation and propagation which results in increase in the rate of polymerization. With increasing dispersion time, more LMA molecule penetrates the intergallery spacing in nanoclay, thus encouraging more interaction between $>C=O$ group and Al-atom in nanoclay and hence promotes the polymerization rate.

Coordination of $>C=O$ group may lower the activation enthalpy of halogen transfer and consequently reduces the apparent propagation activation enthalpy¹⁵. This subsequently increases the dynamic equilibrium constant between radicals and dormant species, thereby encouraging the generation of active radicals in the medium and polymerization rate gets enhanced. Guo et al¹⁷ also reported the ATRP of methacrylate monomers (butyl methacrylate, methyl methacrylate etc.) promoted by aluminium isopropoxide. The enhanced rate of polymerization was explained in terms of coordination between the $>C=O$ group of monomer to aluminium propoxide, a lewis acid¹⁶. In order to verify the coordination between the $>C=O$ group of monomer and nanoclay, controlled polymerization of styrene was carried out via ATRP in the presence of (2 wt %) nanoclay as an additive. In this case there was no significant improvement in polymerization rate compared to the system devoid of nanoclay (65% conversion with 2 wt. % clay; 61% conversion without clay, reaction time=3h.). This strongly confirms the participation of $>C=O$ group of LMA monomer with nanoclay.

This is supported by FTIR spectra [Figure 5] which shows that the carbonyl absorption band of LMA in presence of nano clay as a function of dispersion time (td) is shifted by 8 cm^{-1} (after 10h of dispersion) and 12 cm^{-1} (after 20h of dispersion) towards lower frequency. This indicate that the electron deficient Al in nanoclay interacts with the $>C=O$ group of LMA monomer (shown in reaction scheme 1). This particular interaction tends to decrease the double bond character of the carbonyl group thereby shifting the absorption band to lower frequency.

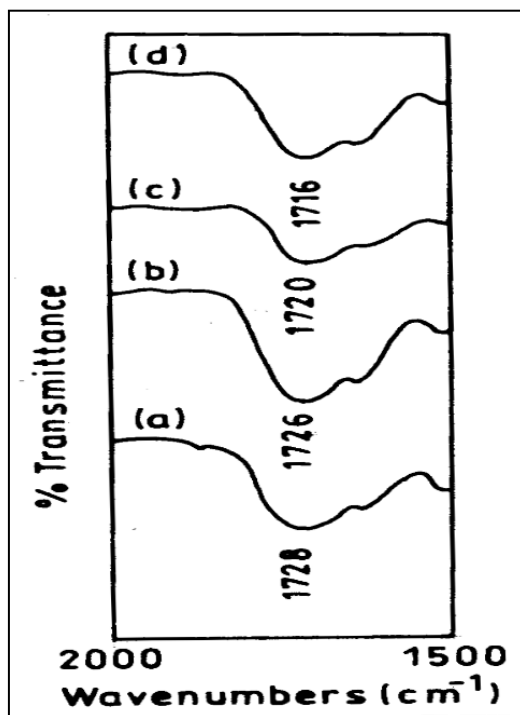


Figure 5: FTIR spectra of LMA monomer in presence of clay dispersed for (a) 0h, (b) 1 h, (c) 10h and (d) 20h

4.5 Molecular Characterization

Molecular weight and molecular weight distribution (PDI) of virgin PLMA and various polymer samples extracted from its nanocomposites prepared by in-situ ATRP, were obtained by GPC analysis. Molecular weight of all the samples display monomodal peak distributions corresponding to a molecular weight value, predetermined by suitable choice of the mole ratio of monomer to initiator.

The samples were targeted to prepare so that they have comparable values of molecular weights. These values are shown in Table 2. Molecular weight obtained from the GPC is higher than the theoretically calculated molecular weight the reason for the higher molecular weight (Mn_{GPC}) observed than calculated could be due to the difference in hydrodynamic volume of PLMA and PS which has been used as calibration standards.

Table.2: Molecular weight and polydispersity indices of neat and extracted PLMA

Sample Designation	Molecular weight ($Mn_{theory} \times 10^{-3}$)	Molecular weight ($Mn_{GPC} \times 10^{-3}$)	Mw/Mn
PLMA-0	6.40	7.43	1.27
PLMA-2[20]	7.68	8.13	1.45
PLMA-4[20]	8.10	9.54	1.68
PLMA-6[20]	8.83	10.02	2.10

V. MORPHOLOGY OF IN-SITU PREPARED NANOCLAY-PLMA COMPOSITE

5.1 WAXD

Figure 6 shows the XRD patterns of nanoclay (Cloisite 30B), PLMA and PLMA nanocomposites having 2, 4 and 6% (wt) nanoclay. It is clear from Figure 5.6 that there is no diffraction peak in the range of $2\theta = 3-10^\circ$ in case of PLMA and PLMA having (2 % and 4 % [w/w]). as opposed to organoclay that have diffraction peak at $2\theta = 4.838^\circ$ (d_{001} spacing=1.82nm).

This suggests the complete delamination of silicate layers dispersed in PLMA matrix. However, a small broad hump was observed in the case of PLMA prepared in presence of 6 % [w/w] nanoclay [PLMA-6]. This may be due to the agglomeration of clay at higher filler loading caused by their poor dispersion in the PLMA matrix.

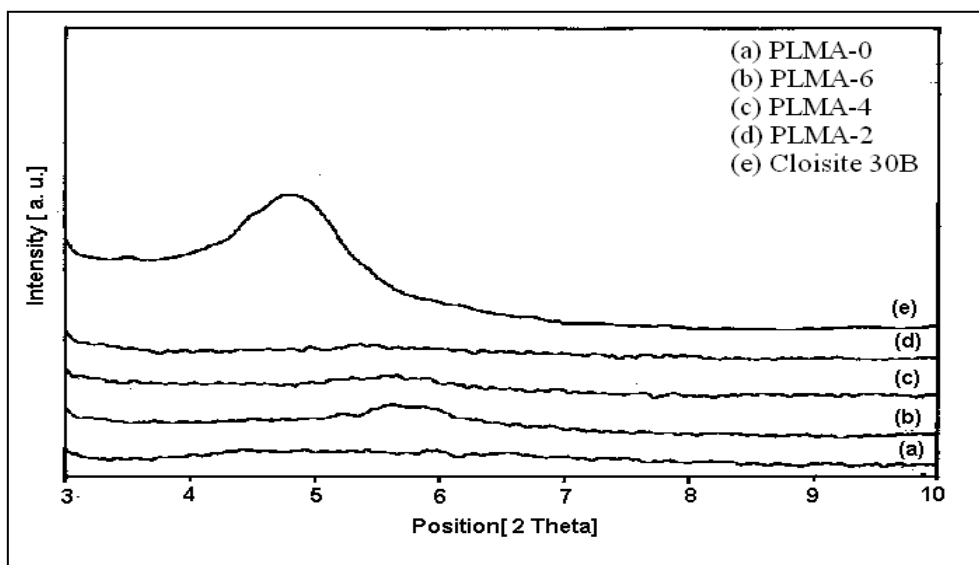


Figure .6: WXRd patterns of PLMA-clay nanocomposites: (a) PLMA-0 ; (b) PLMA-6 ;(c) PLMA-4 ;(d) PLMA-2; (e) Cloisite 30B

5.2 Transmission Electron Micrograph:

The morphology of PLMA/organically modified clay nanocomposites obtained by in-situ ATRP methods have also been analyzed using TEM (Figure 7). The white/grey areas represent the polymer matrix phase and the dark areas represent organoclay. TEM image reveals that there are mostly well-dispersed silicate layers.

The differences in dispersion of clay tactoids in nanocomposites were further examined by Transmission Electron Microscopy (TEM) (Figure 7). The white/grey areas represent the polymer matrix phase and the dark areas represent organoclay. It can be seen from Figure 7. TEM bright field image reveals that there are mostly well-dispersed silicate layers with average interlayer distance. The clay layers are lying at different angular dispositions due to significant distribution of organoclay tactoids. In case of sample PLMA-2, completely exfoliated structure of clay was seen.

This observation is consistent with that obtained from the WAXD pattern shown in Figure 6. A similar type of delaminated morphology is observed in *PLMA-4* (Figure 7-b) which shows both exfoliated and intercalated morphology, whereas in sample *PLMA-6*, clay particles show some local agglomeration (Figure 7-c).

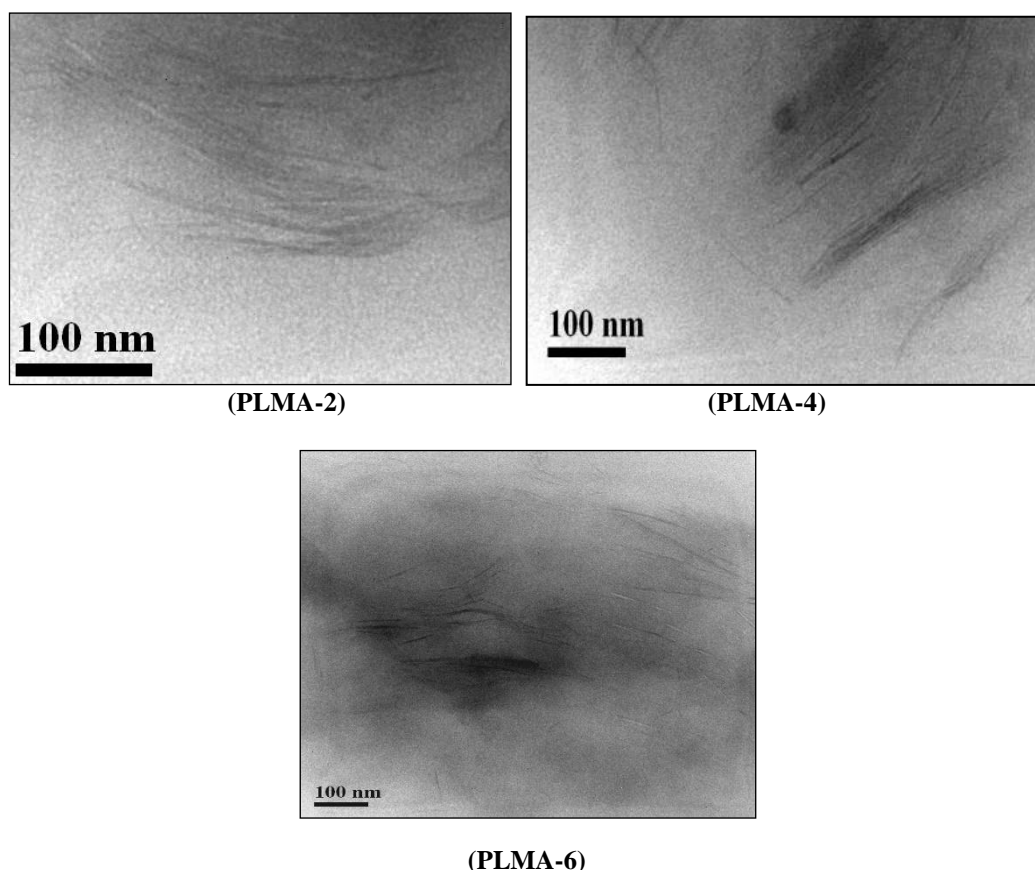


Figure 7: Transmission electron micrograph of PLMA-clay Nanocomposites with varying content of nanoclay (cloisite 30B)

5.3 Thermal Characterization

Figure 8 (a-e) shows the TG/DTG traces of PLMA, PLMA-clay nanocomposite and cloisite 30B.

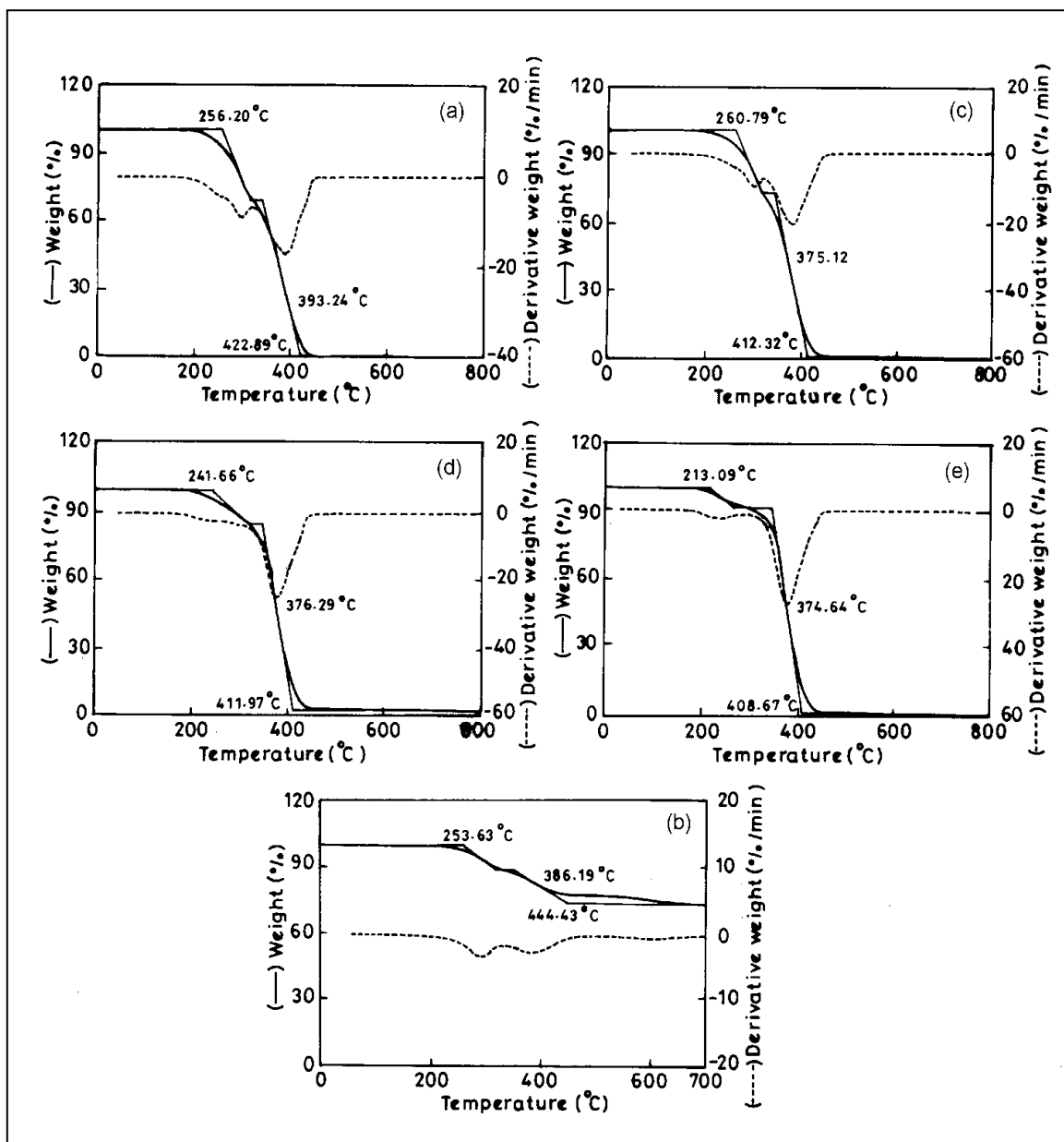


Figure 8: TG/DTG traces of PLMA, Cloisite 30B and PLMA-clay nanocomposites (a) PLMA, (b) Cloisite 30B, (c) PLMA-2, (d) PLMA-4 and (e) PLMA-6

The weight loss due to the formation of volatile products after degradation at high temperature is monitored as a function of temperature. The thermal stability of the PLMA-based nanocomposites showed the two-step degradation. First step random chain scission through pyrolysis of the ester groups, then in the second step, main chain polymer was degraded.

Table 3: Results of thermogravimetric analysis

Sample designation	1 st step degradation			2 nd step degradation		
	Onset	End	Step inflection	Onset	End	Step inflection
Cloisite 30B	253.63	313.75	285.95	346.39	444.43	386.19
PLMA-0	256.20	318.22	294.83	343.07	422.89	393.24
PLMA-2	260.79	314.56	298.90	340.96	412.32	375.12
PLMA-4	241.66	313.45	304.00	340.37	411.97	376.29
PLMA-6	213.09	260.76	241.88	342.81	408.67	374.64

Table 4 shows the % weight loss between two different temperatures e.g. 200-300°C and 300-450°C. Table 4 shows as the amount of nanoclay increases in the polymer % weight loss decreases in the region of 200-300°C. However, in the temperature range of 300-450°C, content of nanoclay had no significant effect on the % weight loss. It is apparent that the nanocomposite with 2% clay content has greater thermal stability than that of neat PLMA and nanocomposite with 4% and 6% clay content. The onsets of degradation as measured from the intersection of the tangent of the initial part are registered in table 3. The corresponding differential curve (DTG) in Figure 8 clearly shows that the thermal degradation is retarded in presence of 2% nanoclay. However in the case of 4% and 6% clay content it follows the degradation pattern of neat PLMA polymer. The reason may be in the case of 2% clay content maximum exfoliation observed that confirm from the TEM analysis which show maximum thermal stability.

Table 4: Percentage weight loss between two different temperatures.

Sample designation	Percentage weight loss between (200-300°C)	Percentage weight loss between (300-450°C)
Cloisite 30B	8.10	22.13
PLMA-0	19.84	77.77
PLMA-2	18.25	78.57
PLMA-4	11.90	84.12
PLMA-6	8.73	88.88

VI. CONCLUSION

A beneficial role of nanoclay as additives in ATRP of LMA was observed as it leads to a remarkable increase in polymerization rate without losing control. Two parameters, viz., the dispersion time of clay in monomer prior to polymerization and extent of clay loading are found to have a positive effect on the kinetics of polymerization. FTIR study demonstrates that there is a definite interaction between the hydroxyl groups of clay and the carbonyl moiety of the dormant species, thereby activating the C-Br bond next to the ester carbonyl bond and hence higher concentration of active radicals. PLMA-clay nanocomposites with predictable molecular weight and polydispersity indices have been prepared at different clay loadings by in-situ atom transfer radical polymerization. WAXD and TEM analysis reveal that the structures of resulting nanocomposites are mostly exfoliated clay morphology.

REFERENCES

- [1] Wang, J.S.; Matyjaszewski, K. *J Am Chem Soc* 1995, 117, 5614.
- [2] Kato, M.; Kamigaito, M.; Sawamoto, M.; Higashimura, T. *Macromolecules* 1995, 28, 1721.
- [3] Wang, X. S.; Luo, N.; Ying, S. K. *J Polym Sci Part A Polym Chem* 1999, 37, 1255.
- [4] Matyjaszewski, K.; Nakagawa, Y.; Jasiiczek, C. B. *Macromolecules* 1998, 31, 1535.
- [5] Wang, X. S.; Armes, S. P.; *Macromolecules* 2000, 33, 6640.
- [6] Chatterjee, U.; Jewrajka, S. K.; Mandal, B. M. *Polymer* 2005, 46, 1575
- [7] Haddleton, D. M.; Heming, A. M.; Kukulj, D.; Duncalf, D. J.; Shooter, A. J. *Macromolecules* 1998, 31, 2016.
- [8] Haddleton, D.M.; Kukulj, D.; Duncalf, D.J.; Heming, A.M.; Shooter, A.J. *Macromolecules* 1998, 31, 5201.
- [9] Matyjaszewski, K.; Patten, T. E.; Xia, J. *J Am Chem Soc* 1997, 119, 674
- [10] Giannelis, E. P. *Adv. Mater* 1996, 8, 29.
- [11] Bottcher, H.; Hallensleben, M. L.; Nuß, S.; Wurm, H.; Bauer, J.; Behrens, P. *J. Matr Chem* 2002, 12, 1351.
- [12] Pluart, D.; Duchet, J.; Sautereau, H.; Halley, P.; Gerard, J-F. *Appl. Clay Sci* 2004, 25, 207.
- [13] Worrall, W. E.; *Clays: their nature, origin and general properties. Maclaren & Sons: London, 1986, pp 50.*
- [14] Kizhakkedathu, J.N.; Brooks, D.E. *Macromolecules* 2003, 36, 591.
- [15] Wada, K. *Clay Miner* 1967, 7, 51.
- [16] Luo, R.; Sen, A. *Macromolecules* 2007, 40, 154.
- [17] GuoHan, Z.; Wu, P. *J Mol Cat Part A Chem* 2000, 159, 77
- [18] Milner, S.T. *Science* 1991, 251, 905.
- [19] Zhao, B.; Brittain, W.J. *Prog Polym Sci* 2000, 25, 677.
- [20] Karesoia, M.; Jokinen, H.; Karalainen, E.; Pulkkinen, P.; Torkkeli, M.; Soininen, A.; Ruokolainen, J.; Tenhu, H. *J. Polym. Sci., Part A: Polym. Chem.* 2009, 47, 3086
- [21] (a) Datta, H.; Singha, N. K.; Bhowmick, A. K. *Macromolecules* 2008, 41, 50. (b) Datta, H.; Bhowmick, A. K.; Singha, N. K. *J. Polym. Sci., Part A: Polym. Chem.* 2008, 46, 5014
- [22] Abdollahi, M.; Ali, M.; Semsarzadeh. *European Polymer Journal* 2009, 45, 85.
- [23] Srivastava, P. K.; Choudhary, V. J. *Appl. Polym. Sci.* 2012, 125, 31-35